Mon. Not. R. Astron. Soc. **000**, 1–**??** (2009) Printed 12 November 2010 (MN LATEX style file v2.2)

Thin accretion discs around millisecond X-ray pulsars

Solomon Belay Tessema[1,2⋆] and Ulf Torkelsson [2]
[1]*Department of Physics,Addis Ababa University, P.O.Box 1176, Addis Ababa, Ethiopia*
[2]*Department of Physics, University of Gothenburg, SE 412 96 Gothenburg, Sweden*

Accepted . Received ; in original form

ABSTRACT
Millisecond x-ray pulsars have weak magnetic dipole moments of $\sim 10^{16}\,\mathrm{T\,m^3}$ compared to ordinary X-ray pulsars with dipole moments of $10^{20}\,\mathrm{T\,m^3}$. For this reason a surrounding accretion disc can extend closer to the neutron star, and thus reach a higher temperature, at which the opacity is dominated by electron scattering and radiation pressure is strong. We compute the self-similar structure of such a geometrically thin axisymmetric accretion disc with an internal dynamo. Such models produce significantly stronger torques on the neutron star than models without dynamos, and can explain the strong spin variations in some millisecond X-ray pulsars.

Key words: accretion, accretion discs – magnetic fields – MHD –stars: magnetic fields – stars: neutron – X-rays:binaries – pulsars: general

1 INTRODUCTION

The first accretion-powered millisecond pulsar, SAX J1808.4-3658, was discovered a decade ago (Wijnands & van der Klis 1998; Chakrabarty & Morgan 1998). Since then several other millisecond X-ray pulsars with spin periods between 1.7 and 5.4 ms have been discovered (e.g. XTE J0929-314, XTE J1751-305, XTE 1807-294 and XTE J1814-338; see Wijnands 2004 for a review). These neutron stars have considerably weaker magnetic dipole moments, $\sim 10^{16}\,\mathrm{T\,m^3}$, than the conventional X-ray pulsars. The accretion disc then extends much closer to the neutron star, where it reaches such a high temperature that the opacity is dominated by electron scattering and radiation pressure can grow stronger than the gas pressure. On the other hand the accretion rates in these systems can be so low that the Alfvén radius might be located outside of the co-rotation radius of the neutron star. Conventionally it has been thought that such systems will eject the mass that is transferred from the companion star through the propeller mechanism (Illarionov & Sunyaev 1975), though it has been pointed out by Spruit & Taam (1993) and Rappaport, Fregeau & Spruit (2004) that the velocity excess right outside the co-rotation radius is insufficient to eject all the matter. Spruit & Taam (1993) found that when the Alfvén radius is only slightly larger than the co-rotation radius then the disc will cycle between one state in which the matter is accumulated outside the co-rotation radius and another state in which it is accreted onto the star. Later Rappaport, Fregeau & Spruit (2004) constructed a steady accretion disc model, in which the entire disc is located outside of the co-rotation radius. The magnetic field of the neutron star is penetrating this disc and is mediating an exchange of angular momentum between the accretion disc and the neutron star as in the model by Ghosh & Lamb (1979). Since the entire accretion disc is rotating more slowly than the neutron star in this case, the disc brakes the rotation of the neutron star.

The models of Ghosh & Lamb (1979) and Rappaport, Fregeau & Spruit (2004) have ignored the possibility of an internal dynamo in the accretion disc, and have considered only the magnetic field that is generated in the disc by the mismatch in the rotation of the neutron star and the disc. However the magnetic field due to a dynamo can strengthen the coupling between the accretion disc and the neutron star, and we (Tessema & Torkelsson 2010) have shown that the angular momentum exchange between the accretion disc and the neutron star can increase by more than an order of magnitude compared to the standard model by Ghosh & Lamb (1979). Furthermore the dynamo is insensitive to the rotation of the neutron star, and can therefore in principle provide a spin-up torque even at a low accretion rate.

A complementary approach to study the magnetic interaction between an accretion disc and a star is represented by the numerical simulations by Long et al. (2008). In these simulations it is possible to study more complicated magnetic field geometries than are accessible to semi-analytic studies (see for instance Long et al. 2008), but the resolution is so low that it is not possible to study the appearance of small-scale turbulence and the resulting turbulent transport and dynamo action in the simulation. Thus these simulations do not really address the viability of a dynamo in the disc. However there are other things one can learn from these simulations. They show how the matter is streaming via funnel flows from the accretion disc onto the magnetic poles of the neutron star. Furthermore they show that angular momentum is also lost from the accretion disc through the jets that are accelerated away from the disc. Romanova et al. (2009) make a distinction between a conical jet that transport most of the mass, and a less dense axial jet inside the conical jet. The latter component can dominate the energetics if the star is in the

⋆ E-mail: newtonsolbel@yahoo.com; torkel@physics.gu.se

propeller regime. It is also noteworthy that these simulations confirm that some matter might still be accreted when the star is in the propeller regime.

The purpose of this paper is to extend our previous study (Paper I) of an accretion disc with an internal dynamo around a magnetised star to the discs around millisecond pulsars. The difference is that due to the weak magnetic field the disc extends to much smaller radii, at which it becomes so hot that a significant part of the opacity is due to electron scattering, and radiation pressure might dominate over the gas pressure. Therefore in the spirit of Shakura & Sunyaev (1973, 1976) we divide the disc into an outer region with gas pressure and free-free opacity, a middle region with gas pressure and electron scattering opacity, and an inner region with radiation pressure and electron scattering.

In Sect. 2 we derive a single ordinary differential equation, which is generally applicable for the radial structure of the accretion disc independently of the equation of state and the form of the opacity. We then introduce the equations of state and the opacity prescriptions for the different regions of the disc in Sect. 3 and present the numerical solutions in Sect. 4. The properties of these solutions and their application to the millisecond X-ray pulsars are discussed in Sect. 5, and we finally summarise our results in Sect. 6.

2 GOVERNING EQUATIONS

2.1 The magnetohydrodynamic angular momentum balance

Our approach is an extension of the standard model for a thin accretion disc (Shakura & Sunyaev 1973), and it follows closely the method that we introduced in Paper I, though we will now consider a general opacity law and equation of state. For this reason we only summarise the steps leading up to Eq. (21) of Paper I, after which we deviate from the treatment in Paper I.

The surface density of the accretion disc is defined as

$$\Sigma = \int_{-\infty}^{\infty} \rho \mathrm{d}z = 2\rho H, \tag{1}$$

where ρ is the density, and H the half thickness of the disc. We can then write the accretion rate as

$$\dot{M} = -2\pi R \Sigma v_R, \tag{2}$$

which is independent of the radial coordinate R, and where v_R is the radial velocity.

A thin accretion disc is supported by the centrifugal force in the radial direction, so we get that

$$v_\phi^2 - \frac{GM}{R} = 0, \tag{3}$$

where v_ϕ is the azimuthal velocity, G the gravitational constant and M is the mass of the accretor. This shows that the disc rotates in a Keplerian fashion.

The disc is in hydrostatic equilibrium in the vertical direction, which gives us that the pressure at the midplane of the disc is

$$P = \frac{1}{2} H \Sigma \frac{GM}{R^3} = \rho \frac{GMH^2}{R^3} \tag{4}$$

but the hydrostatic equilibrium can also be expressed as

$$\frac{H}{R} = \frac{c_\mathrm{s}}{v_\mathrm{kepl}} \tag{5}$$

where

$$c_\mathrm{s} = \left(\frac{P}{\rho}\right)^{1/2} \tag{6}$$

is the isothermal speed of sound. This shows that the Keplerian velocity is highly supersonic in a thin accretion disc.

The conservation of angular momentum leads to the following height-integrated equation (Paper I)

$$\Sigma \left(v_R \frac{\mathrm{d}l}{\mathrm{d}R} \right) = \left[\frac{B_z B_\phi}{\mu_0} \right]_{-H}^{H} R + \frac{1}{R} \frac{\mathrm{d}}{\mathrm{d}R} \left[R^3 \nu \Sigma \frac{\mathrm{d}}{\mathrm{d}R} \left(\frac{l}{R^2} \right) \right], \tag{7}$$

where the specific angular momentum $l = R v_\phi \propto R^{1/2}$ and ν is the viscosity. The magnetic term describes the exchange of angular momentum between the disc and the star via the magnetosphere. We assume that the vertical magnetic field is due to the dipolar field of the neutron star, so that its value in the equatorial plane is

$$B_\mathrm{z} = -\frac{\mu}{R^3} \tag{8}$$

where μ is the magnetic dipole moment of the star. There are two sources for B_ϕ. The shear between the Keplerian disc and the magnetosphere produces a field whose value in the upper half of the disc is

$$B_{\phi,\mathrm{shear}} = -\gamma B_z \left(1 - \frac{\Omega_\mathrm{s}}{\Omega_\mathrm{k}} \right), \tag{9}$$

where $\Omega_\mathrm{k} = v_\phi / R$, Ω_s is the angular velocity of the star, and γ is a dimensionless parameter of the order of a few (Ghosh & Lamb 1979).

The magnetohydrodynamical turbulence in the accretion disc is also generating a magnetic field, $B_{\phi,\mathrm{dyn}}$, through a dynamo action (see for instance Balbus & Hawley 1998). In order to estimate the strength of this magnetic field we start by making the assumptions that the turbulence is not affected by $B_{\phi,\mathrm{shear}}$, which is justified because in general $|B_{\phi,\mathrm{turb}}| > |B_{\phi,\mathrm{shear}}|$ (Tessema & Torkelsson 2010), and that the accretion is driven in its entirety by the small-scale turbulent magnetic (Maxwell) stress. The latter assumption ignores the fact that the Reynolds stress is responsible for roughly 20% of the radial transport of angular momentum (Brandenburg et al. 1995), but this results in only a minor quantitative change. It is then the $R\phi$-component of the turbulent Maxwell stress tensor, $\langle B_{R,\mathrm{turb}} B_{\phi,\mathrm{turb}} \rangle / \mu_0$, that transports the angular momentum, and we couple this to the pressure in the disc through the Shakura & Sunyaev (1973) α_ss-prescription

$$f_{R\phi} = \frac{-\left\langle B_{R,\mathrm{turb}} B_{\phi,\mathrm{turb}} \right\rangle}{\mu_0} = \alpha_\mathrm{ss} P(r). \tag{10}$$

Note that a negative Maxwell stress means that the angular momentum is transported outwards and that numerical simulations suggest that $\alpha_\mathrm{ss} \sim 10^{-2}$ (Hawley et al. 1995; Brandenburg et al. 1995). Torkelsson (1998) suggested that[1]

$$\gamma_\mathrm{dyn} = \frac{\left\langle B_{\phi,\mathrm{turb}}^2 \right\rangle}{-\left\langle B_{R,\mathrm{turb}} B_{\phi,\mathrm{turb}} \right\rangle}, \tag{11}$$

where $\gamma_\mathrm{dyn} \sim 10$ based on the numerical simulations by Brandenburg et al. (1995). We now assume that due to an inverse cascade this turbulent filed contains a large-scale field, $B_{\phi,\mathrm{dyn}}$ (Frisch, Pouquet, Leorat & Mazure 1975), and we express the ratio of the large-scale field to the rms-value of the turbulent field as

[1] This is a more precise definition of γ_dyn than $B_\phi = \gamma_\mathrm{dyn} B_r$ that was used by Torkelsson (1998).

$$\epsilon = \frac{B_{\phi,\rm dyn}}{\left\langle B^2_{\phi,\rm turb}\right\rangle^{1/2}}. \quad (12)$$

Thus we can express the large-scale magnetic field, that couples to the magnetic field of the neutron star, as

$$B_{\phi,\rm dyn} = \epsilon\left(\alpha_{\rm ss}\mu_0\gamma_{dyn}P(r)\right)^{1/2}, \quad (13)$$

where $-1 \leq \epsilon \leq 1$, and a negative value describes a magnetic field which is pointing in the negative ϕ-direction at the upper disc surface. We will in general be conservative and assume that $|\epsilon| \leq 0.1$, but the simulations by Brandenburg et al. (1995) suggest that $|\epsilon|$ can be significantly larger.

We can now re-express Eq. (7) as

$$\Sigma\left(\nu_R\frac{{\rm d}l}{{\rm d}R}\right) = 2\epsilon\frac{B_z}{\mu_0}\left(\alpha_{\rm ss}\mu_0\gamma_{\rm dyn}P(r)\right)^{1/2}R - 2\gamma\frac{B_z^2}{\mu_0}\frac{(\Omega_{\rm k}-\Omega_{\rm s})}{\Omega_{\rm k}}R + \frac{1}{R}\frac{\rm d}{{\rm d}R}\left[R^3\nu\Sigma\frac{\rm d}{{\rm d}R}\left(\frac{l}{R^2}\right)\right]. \quad (14)$$

which can be formulated as an ordinary differential equation in $\nu\Sigma$ (Paper I).

2.2 Heating and radiative transport

For a slow inflow of matter through an optically thick disc the local viscous dissipation $\mathbf{v}\cdot\mathbf{f}_\nu$ is balanced by the radiative losses $\nabla\cdot\mathbf{F}_{\rm rad}$. This leads to the height-integrated equation

$$\frac{4\sigma T_{\rm c}^4}{3\tau} = \frac{9}{8}\nu\Sigma\frac{GM}{R^3}, \quad (15)$$

where $T_{\rm c}$ is the temperature at the midplane of the disc, σ the Stefan-Boltzmann constant, and the optical depth of the disc is given by:

$$\tau = \int_0^H \kappa\rho dz = \rho H\kappa = \frac{1}{2}\Sigma\kappa, \quad (16)$$

where κ is the sum of the electron scattering opacity

$$\kappa_{\rm es} = 0.04\ {\rm m^2\,kg^{-1}}, \quad (17)$$

and the free-free opacity, which is given by Kramer's law

$$\kappa_{\rm ff} = \kappa_0\rho T_{\rm c}^{-7/2}{\rm m^2\,kg^{-1}} \quad (18)$$

with

$$\kappa_0 = 5\times10^{20}\ {\rm m^5\,kg^{-2}\,K^{7/2}}. \quad (19)$$

Combining Eqs. (14) and (15), we get

$$T_{\rm c}^4 = \frac{27}{32\sigma}\rho H(\kappa_R+\kappa_{es})\nu\Sigma\frac{GM}{R^3} \quad (20)$$

2.3 The vertical structure of an accretion disc

The total pressure is the sum of gas and radiation pressure

$$P(\rho,T_{\rm c}) = \frac{\rho k_{\rm B}T_{\rm c}}{m_{\rm p}\bar{\mu}} + \frac{4\sigma T_{\rm c}^4}{3c} \quad (21)$$

where $k_{\rm B}$ is Boltzmann's constant, $\bar{\mu} = 0.62$ the mean molecular weight for a fully ionised gas, $m_{\rm p}$ the mass of a proton, and c the speed of light, but the pressure can also be expressed using Eq. (4) for hydrostatic equilibrium. We can thus express the scale height in terms of the total pressure

$$H = \left(\frac{k_{\rm B}T_{\rm c}R^3}{m_{\rm p}\bar{\mu}GM} + \frac{4\sigma T_{\rm c}^4R^3}{3c\rho GM}\right)^{1/2}. \quad (22)$$

The viscous stress tensor (Paper 1, Eq. 30) gives us

$$f_{R\phi} = \frac{3}{4}\frac{\Sigma\nu}{H}\left(\frac{GM}{R^3}\right)^{1/2} = \alpha_{\rm ss}P, \quad (23)$$

but pressure and density are related according to Eq. (4), so we can solve for the density of the gas

$$\rho = \frac{3}{4\alpha_{\rm ss}}\frac{\nu\Sigma}{H^3}\left(\frac{GM}{R^3}\right)^{-1/2}. \quad (24)$$

Combining Eqs. (4), (14) and (24) and using $y = \nu\Sigma$ we get

$$\frac{dy}{dR} = \frac{\dot{M}}{6\pi R} - \frac{y}{2R} - \epsilon\left[\frac{4\mu^2\gamma_{dyn}y}{3\mu_0HR^{3/2}}\right]^{1/2}(GM)^{-1/4}R^{-3/2} - \frac{4\mu^2\gamma}{3\mu_0\sqrt{GM}}R^{-9/2}\left[1-\left(\frac{R}{R_{\rm c}}\right)^{3/2}\right], \quad (25)$$

where

$$R_{\rm c} = \left(\frac{GMP_{\rm spin}^2}{4\pi^2}\right)^{1/3} \simeq 1.5\times10^6P_{\rm spin}^{2/3}M_1^{1/3}\,{\rm m}, \quad (26)$$

is the co-rotation radius, at which the Keplerian angular velocity is the same as the stellar angular velocity. Here $P_{\rm spin} = \frac{2\pi}{\Omega_{\rm s}}$ is the spin period of the star and $M_1 = \frac{M}{M_\odot}$. As $R\to\infty$

$$y \to \frac{\dot{M}}{3\pi},$$

which we use as the outer boundary condition.

We now introduce the dimensionless variable Λ through

$$y = \Lambda\dot{M}, \quad (27)$$

and a dimensionless radial coordinate through

$$R = rR_{\rm A}, \quad (28)$$

where $R_{\rm A}$ is the Alfvén radius, which is given by setting the magnetic pressure equal to the ram pressure (e.g. Shapiro & Teukolsky 1983)

$$R_{\rm A} = \left(\frac{2\pi^2\mu^4}{GM\dot{M}^2\mu_0^2}\right)^{1/7} \simeq 1.4\times10^4\dot{M}_{14}^{-2/7}M_1^{-1/7}\mu_{16}^{4/7}{\rm m}, \quad (29)$$

where $\dot{M}_{14}$ represents the mass transfer rate in units of $10^{14}\,{\rm kg\,s^{-1}}$, and μ_{16} is the stellar magnetic moment in units of $10^{16}\,{\rm T\,m^3}$. The Alfvén radius should not be taken as the location of the inner edge of our discs, since this is a quantity that comes out of our solutions, but merely as a convenient length unit. Furthermore we introduce the fastness parameter

$$\omega_{\rm s} = \left(\frac{R_A}{R_{\rm c}}\right)^{3/2} = 0.36M_1^{-5/7}\dot{M}_{14}^{-3/7}\mu_{16}^{6/7}\left(\frac{P_{\rm spin}}{4.8\,{\rm ms}}\right)^{-1}. \quad (30)$$

We can now write Eq. (25) as:

$$\frac{d\Lambda}{dr} = \frac{1}{6\pi r} - \frac{\Lambda}{2r} - \epsilon\left[\frac{4\mu^2\gamma_{dyn}\Lambda}{3\mu_0H\dot{M}}\right]^{1/2}(GM)^{-1/4}R_A^{-5/4}r^{-9/4} - \frac{4\mu^2\gamma}{3\mu_0\sqrt{GM\dot{M}}}R_A^{-7/2}r^{-9/2}\left[1-\omega_{\rm s}r^{3/2}\right], \quad (31)$$

3 REGIONAL DISC STRUCTURE EQUATIONS

In order to solve Eq. (31) numerically we need to determine H for the different regions in the disc. With gas pressure and Kramer's opacity we get

$$H(r) = \left(\frac{243\kappa_0}{512\sigma}\right)^{1/20} \alpha_{\rm ss}^{-1/10} \left(\frac{k_{\rm B}(rR_{\rm A})^3}{m_p\bar{\mu}GM}\right)^{3/8} \left(\dot{M}\Lambda\right)^{3/20}, \quad (32)$$

and for the gas pressure and electron scattering opacity

$$H(r) = \left(\frac{81\kappa_{\rm es}}{128\sigma\alpha_{\rm ss}}\right)^{1/10} \left(\frac{k_{\rm B}}{m_p\bar{\mu}}\right)^{2/5} \left(\frac{(rR_{\rm A})^3}{GM}\right)^{7/20} \left(\dot{M}\Lambda\right)^{1/5}. \quad (33)$$

Finally with radiation pressure and electron scattering the scale height is

$$H = \frac{9\kappa_{\rm es}}{8c}\nu\Sigma = \frac{9\kappa_{\rm es}}{8c}(\dot{M}\Lambda) \quad (34)$$

which is essentially independent of R. This comes from the fact that for radiation pressure $T_{\rm c}^4 \sim \nu\Sigma^2 MR^{-3}$.

We can now write down the self-similar structure of the different regions of the accretion disc in terms of the function $\Lambda(r)$. The toroidal magnetic field is given by the same expression

$$B_{\phi,\,\rm shear} = -3.6\times10^3\gamma M_1^{3/7}\dot{M}_{14}^{6/7}\mu_{16}^{-5/7}\left(1-\omega_s r^{3/2}\right)r^{-3}{\rm T} \quad (35)$$

everywhere in the disc, but for all other quantities we have to handle the different regions of the disc separately.

In the outer disc where $P_{\rm g} \gg P_{\rm rad}$, and $\kappa_{\rm ff} \gg \kappa_{\rm es}$ we have that:

$$\Sigma = 1.6\times10^6\bar{\mu}^{3/4}\alpha_{\rm ss}^{-4/5}M_1^{5/14}\dot{M}_{14}^{32/35}\mu_{16}^{-3/7}\Lambda(r)^{7/10}r^{-3/4}{\rm kg\,m^{-2}} \quad (36)$$

$$T_{\rm c} = 8.1\times10^7\bar{\mu}^{1/4}\alpha_{\rm ss}^{-1/5}M_1^{5/14}\dot{M}_{14}^{18/35}\mu_{16}^{-3/7}\Lambda(r)^{3/10}r^{-3/4}{\rm K} \quad (37)$$

$$\frac{H}{R} = 8.1\times10^{-3}\bar{\mu}^{-3/8}\alpha_{\rm ss}^{-1/10}M_1^{-11/28}\dot{M}_{14}^{4/35}\mu_{16}^{1/14}\Lambda(r)^{3/20}r^{1/8} \quad (38)$$

$$\rho_{\rm c} = 7.1\times10^3\bar{\mu}^{9/8}\alpha_{\rm ss}^{-7/10}M_1^{25/28}\dot{M}_{14}^{38/35}\mu_{16}^{-15/14}\Lambda(r)^{11/20}r^{-15/8}{\rm kg\,m^3} \quad (39)$$

$$\tau = 5.9\times10^2\bar{\mu}\alpha_{\rm ss}^{-4/5}\dot{M}_{14}^{1/5}\Lambda(r)^{1/5} \quad (40)$$

$$\nu = 6.4\times10^7\bar{\mu}^{-3/4}\alpha_{\rm ss}^{4/5}M_1^{-5/14}\dot{M}_{14}^{3/35}\mu_{16}^{3/7}\Lambda(r)^{3/10}r^{3/4}{\rm m^2\,s^{-1}} \quad (41)$$

$$v_R = 7.4\times10^2\bar{\mu}^{-3/4}\alpha_{\rm ss}^{4/5}M_1^{-3/14}\dot{M}_{14}^{13/35}\mu_{16}^{-1/7}\Lambda(r)^{-7/10}r^{-1/4}{\rm m\,s^{-1}} \quad (42)$$

$$B_{\phi,\rm dyn} = 7.7\times10^4\epsilon\bar{\mu}^{3/16}\gamma_{\rm dyn}^{1/2}\alpha_{\rm ss}^{1/20}M_1^{5/8}\dot{M}_{14}^{4/5}\mu_{16}^{-3/4}\Lambda(r)^{17/40}r^{-21/16}{\rm T} \quad (43)$$

The transition from the outer to the middle region occurs where $\kappa_{\rm es} = \kappa_{\rm ff}$. Assuming that $\Lambda \simeq 1/3\pi$ at this point we have that the transition radius is

$$r_{OM} = 47\bar{\mu}^{-1/3}M_1^{10/21}\dot{M}_{14}^{20/21}\mu_{16}^{-4/7},$$

which is independent of $\alpha_{\rm ss}$.

In the middle disc, where $P_{\rm g} \gg P_{\rm rad}$, and $\kappa_{\rm es} \gg \kappa_{\rm ff}$, we have that:

$$\Sigma = 7.1\times10^5\bar{\mu}^{4/5}\alpha_{\rm ss}^{-4/5}M_1^{2/7}\dot{M}_{14}^{27/35}\mu_{16}^{-12/35}\Lambda(r)^{3/5}r^{-3/5}{\rm kg\,m^{-2}} \quad (44)$$

$$T_{\rm c} = 1.8\times10^8\bar{\mu}^{1/5}\alpha_{\rm ss}^{-1/5}M_1^{3/7}\dot{M}_{14}^{23/35}\mu_{16}^{-18/35}\Lambda(r)^{2/5}r^{-9/10}{\rm K} \quad (45)$$

$$\frac{H}{R} = 1.2\times10^{-2}\bar{\mu}^{-2/5}\alpha_{\rm ss}^{-1/10}M_1^{-5/14}\dot{M}_{14}^{13/70}\mu_{16}^{1/35}\Lambda(r)^{1/5}r^{1/20} \quad (46)$$

$$\rho_{\rm c} = 2.0\times10^3\bar{\mu}^{6/5}\alpha_{\rm ss}^{-7/10}M_1^{11/14}\dot{M}_{14}^{61/70}\mu_{16}^{-33/35}\Lambda(r)^{2/5}r^{-33/20}{\rm kg\,m^{-3}} \quad (47)$$

$$\tau = 1.4\times10^4\bar{\mu}^{13/10}\alpha_{\rm ss}^{-4/5}M_1^{2/7}\dot{M}_{14}^{27/35}\mu_{16}^{3/35}\Lambda(r)^{3/5}r^{-3/5} \quad (48)$$

$$\nu = 1.5\times10^8\bar{\mu}^{-4/5}\alpha_{\rm ss}^{4/5}M_1^{-2/7}\dot{M}_{14}^{8/35}\mu_{16}^{12/35}\Lambda(r)^{2/5}r^{3/5}{\rm m^2\,s^{-1}} \quad (49)$$

$$v_R = 1.6\times10^3\bar{\mu}^{-4/5}\alpha_{\rm ss}^{4/5}M_1^{-1/7}\dot{M}_{14}^{18/35}\mu_{16}^{-8/35}\Lambda(r)^{-3/5}r^{-2/5}{\rm m\,s^{-1}} \quad (50)$$

$$B_{\phi,\rm dyn} = 6.3\times10^4\epsilon\bar{\mu}^{1/5}\gamma_{\rm dyn}^{1/2}\alpha_{\rm ss}^{1/20}M_1^{17/28}\dot{M}_{14}^{107/140}\mu_{16}^{-51/70}\Lambda(r)^{2/5}r^{-51/40}{\rm T} \quad (51)$$

The disc structure changes drastically in the inner disc where $P_{\rm rad} \gg P_{\rm g}$ and $\kappa_{\rm es} \gg \kappa_{\rm ff}$, where we have that

$$\Sigma = 9.6\times10^1\alpha_{\rm ss}^{-1}M_1^{-5/7}\dot{M}_{14}^{-10/7}\mu_{16}^{6/7}\Lambda(r)^{-1}r^{3/2}{\rm kg\,m^{-2}} \quad (52)$$

$$T_{\rm c} = 1.9\times10^7\alpha_{\rm ss}^{-1/4}M_1^{5/28}\dot{M}_{14}^{3/28}\mu_{16}^{-3/14}r^{-3/8}{\rm K} \quad (53)$$

$$\frac{H}{R} = 1.1M_1^{1/7}\dot{M}_{14}^{9/7}\mu_{16}^{-4/7}\Lambda(r)r^{-1} \quad (54)$$

$$\rho_{\rm c} = 3.2\times10^{-3}\alpha_{\rm ss}^{-1}M_1^{-5/7}\dot{M}_{14}^{-17/7}\mu_{16}^{6/7}\Lambda(r)^{-2}r^{3/2}{\rm kg\,m^{-3}} \quad (55)$$

$$\tau_{es} = 1.9\alpha_{\rm ss}^{-1}M_1^{-5/7}\dot{M}_{14}^{-10/7}\mu_{16}^{6/7}\Lambda(r)^{-1}r^{3/2} \quad (56)$$

$$\nu = 1.0\times10^{12}\alpha_{\rm ss}M_1^{5/7}\dot{M}_{14}^{17/7}\mu_{16}^{-6/7}\Lambda(r)^2r^{-3/2}{\rm m^2\,s^{-1}} \quad (57)$$

$$v_R = 1.2\times10^7\alpha_{\rm ss}M_1^{6/7}\dot{M}_{14}^{19/7}\mu_{16}^{-10/7}\Lambda(r)r^{-5/2}{\rm m\,s^{-1}} \quad (58)$$

$$B_{\phi,\rm dyn} = 6.6\times10^3\epsilon\gamma_{\rm dyn}^{1/2}\alpha_{\rm ss}^{1/20}M_1^{5/14}\dot{M}_{14}^{3/14}\mu_{16}^{-3/7}r^{-3/4}{\rm T} \quad (59)$$

It is of particular significance here that $\Sigma \propto \Lambda^{-1}$.

The transition radius between the middle and the inner region is estimated by equating the gas and radiation pressures in the middle region and approximating Λ with $1/3\pi$

$$r_{IM} = 12\bar{\mu}^{8/21}\alpha_{\rm ss}^{2/21}M_1^{10/21}\dot{M}_{14}^{22/21}\mu_{16}^{-4/7}$$

We then see that the accretion disc right outside of the Alfvén radius is dominated by radiation pressure only if

$$\mu_{16} < 83\bar{\mu}^{2/3}\alpha_{\rm ss}^{1/6}M_1^{5/6}\dot{M}_{14}^{11/6} \quad (60)$$

This condition is not fulfilled for a conventional X-ray pulsar with a magnetic dipole moment of $\sim 10^{20}\,{\rm T\,m^3}$ (White & Stella 1988), though it can be fulfilled for a millisecond X-ray pulsar.

4 GLOBAL SOLUTIONS

For our fiducial model we take a neutron star of $M = 1.4M_\odot$ with a magnetic moment of $10^{16}\,{\rm T\,m^3}$ and a spin period of 4.8 ms. We set the dimensionless parameters γ and $\gamma_{\rm dyn}$ to 1 and 10, respectively, while $\alpha_{\rm ss} = 0.01$. γ, $\gamma_{\rm dyn}$, and $\alpha_{\rm ss}$ appear only in combinations with other parameters, and thus their values do not carry any special significance, but the parameters ϵ and $\dot{M}$ appear on their own in the equation, and therefore influence the solution in unique ways. In particular $\dot{M}$ influences the fastness parameter and the transition radii between the regions of the accretion disc. In this paper we consider three different accretion rates, $\dot{M}_{14} = 0.012$, 0.12 and 1.5. We list the corresponding fastness parameters and transition radii in Tab. 1.

4.1 Case I: $R_{\rm A} > R_{\rm OM}$

The accretion disc consists of only an outer region when $r_{\rm OM} < 1$, which corresponds to that $\dot{M} < 1.4\times10^{12}\,{\rm kg\,s^{-1}}$ for our fiducial model. Assuming $\dot{M} = 0.012\dot{M}_{14}$ we get the solutions from the top to the bottom of Fig. 1 for $\epsilon = 0.1$, 0.05, 0, −0.05 and −0.1. We see here that $\Lambda \to 0$ at a finite r for $\epsilon = -0.1$, and −0.05, which we called case D in Paper I, since $\rho \to 0$ at this radius (Fig. 2). In the other cases Λ grows without a bound for decreasing r, which we call case V in Paper I, since then the viscous flux of angular

Table 1. The Alfvén radius, fastness parameter ω_s and the transition radii in units of the Alfvén radius for different accretion rates $\dot{M}_{14}$ and the fiducial neutron star.

$\dot{M}_{14}$	R_A [m]	ω_s	r_{OM}	r_{MI}
0.012	4.7×10^4	0.98		
0.12	2.4×10^4	0.37	8.5	–
0.8	1.4×10^4	0.31	52	6.0
1.5	1.2×10^4	0.12	95	12

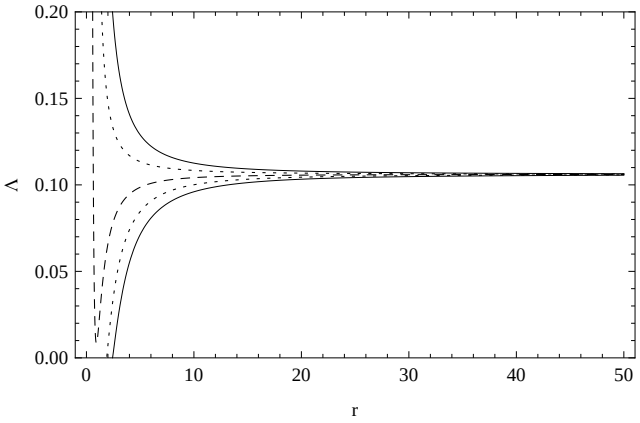

Figure 1. $\Lambda(r)$ for our fiducial neutron star with an accretion rate of $1.2 \times 10^{12}\,\mathrm{kg\,s^{-1}}$, and $\epsilon = 0.1,\ 0.05,\ 0,\ -0.05,\ -0.1$ from the top to the bottom. In this case the disc consists of only an outer region that is dominated by gas pressure and Kramer's opacity.

momentum changes sign at a finite radius where $\frac{\mathrm{d}}{\mathrm{d}r}(\sqrt{r}\Lambda) = 0$ (Fig. 3), which we take as the inner edge of the disc. Inside of this radius the accretion flow is driven by the magnetic coupling to the neutron star.

4.2 Case II: $R_{IM} < R_A < R_{OM}$

The disc has both an outer and a middle region when $0.014 < \dot{M}_{14} < 0.14$. We then use the analytical solution with $\Lambda = 1/3\pi$ for the outer region and solve Eq. (31) numerically for the middle region. For our calculations we take $\dot{M} = 1.2 \times 10^{13}\,\mathrm{kg\,s^{-1}}$, which yields $r_{OM} \approx 8.5$. The numerical solutions for the middle region are shown in Fig. 4 for our fiducial neutron star with $\epsilon = 0.1,\ 0.05,\ 0,\ -0.05,$ and -0.1. We find a case D inner boundary for $\epsilon = -0.1$, while the other solutions have case V inner boundaries. The transition from case D to case V at the ϵ, that gives the smallest possible radius for the inner edge of the disc, which varies weakly with the accretion rate $\dot{M}$.

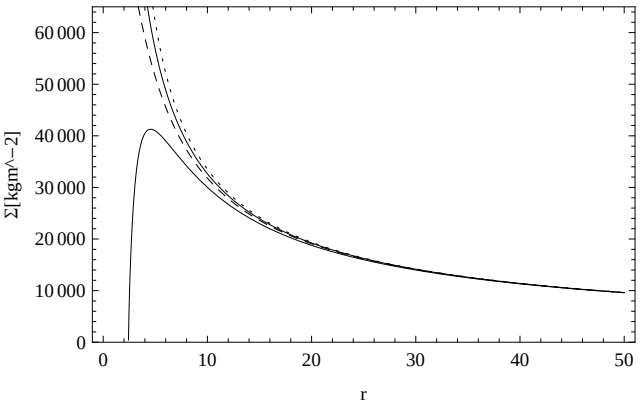

Figure 2. Σ as a function of r for our fiducial neutron star with an accretion rate of $1.2 \times 10^{12}\,\mathrm{kg\,s^{-1}}$, and with $\epsilon = 0.1,\ 0.05,\ 0,$ and -0.1 from the top to the bottom.

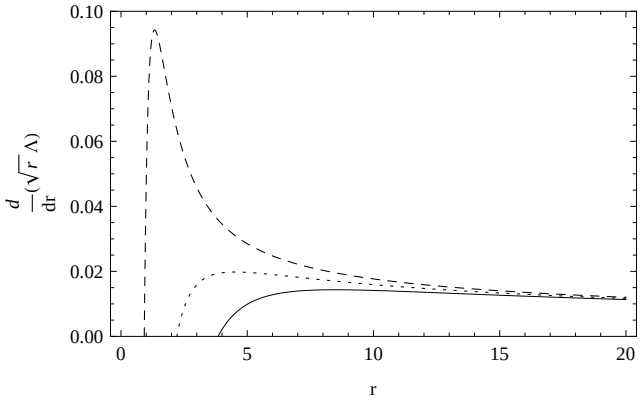

Figure 3. $\frac{d}{dr}\left(\sqrt{r}\Lambda\right)$ as a function of r for the fiducial neutron star with an accretion rate of $1.2 \times 10^{12}\,\mathrm{kg\,s^{-1}}$, and with $\epsilon = 0.1,\ 0.05,$ and 0 from the bottom to the top.

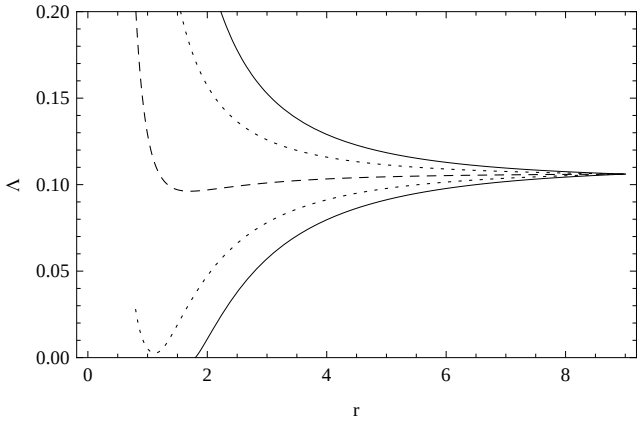

Figure 4. $\Lambda(r)$ for the middle region of an accretion disc around our fiducial neutron star with an accretion rate of $1.2 \times 10^{13}\,\mathrm{kg\,s^{-1}}$, and with $\epsilon = 0.1,\ 0.05,\ 0,\ -0.05,\ -0.1$ from the top to the bottom.

4.3 Case III: $R_A < R_{IM}$

The innermost region of the disc is dominated by radiation pressure and electron scattering when $\dot{M}_{14} > 0.14$. We use two different accretion rates that fulfill this condition, $\dot{M} = 8 \times 10^{13}\,\mathrm{kg\,s^{-1}}$ and $\dot{M} = 1.5 \times 10^{14}\,\mathrm{kg\,s^{-1}}$ together with our fiducial neutron star in our calculations. We assume that $\Lambda = 1/3\pi$ in the outer and middle regions of the disc, and solve Eq. (31) for the inner region starting from $r_{IM} \approx 12$. Our solutions for the inner disc region at the higher accretion rate and with $\epsilon = 0.1,\ 0.05,\ 0,\ -0.05,\ -0.1,$ and -0.12 are shown in Fig. 5. All these solutions have case V inner boundaries except the $\epsilon = -0.12$ model. However because $\Sigma \propto \Lambda^{-1}$ in this case we see that the density goes to infinity at the inner edge of

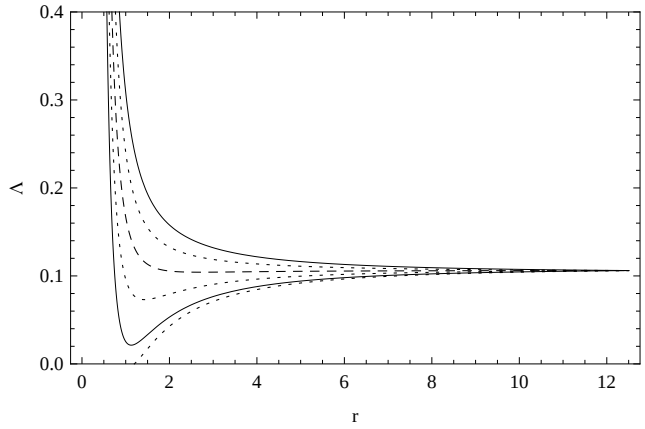

Figure 5. $\Lambda(r)$ for our fiducial neutron star with an accretion rate of $1.5 \times 10^{14}\,\mathrm{kg\,s^{-1}}$, and with $\epsilon = 0.1,\ 0.05,\ 0,\ -0.05,\ -0.1,\ -0.12$ from the top to the bottom.

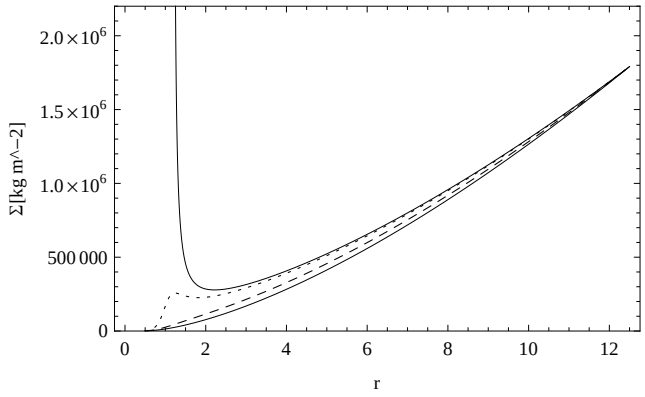

Figure 6. Σ as a function of r for the fiducial neutron star with an accretion rate of $1.5 \times 10^{14}\,\mathrm{kg\,s^{-1}}$, and with $\epsilon = 0.1,\ 0,\ -0.1,$ and -0.12 from the bottom to the top.

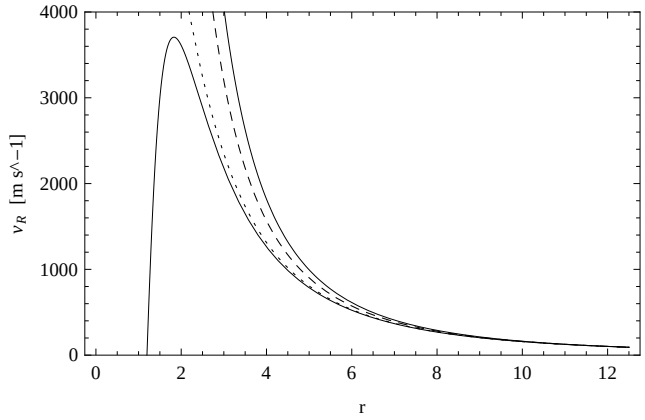

Figure 7. V_R as a function of r for the fiducial neutron star with an accretion rate of $1.5 \times 10^{14}\,\mathrm{kg\,s^{-1}}$ and $\epsilon = 0.1,\ 0,\ -0.1$ and -0.12 from the top to the bottom

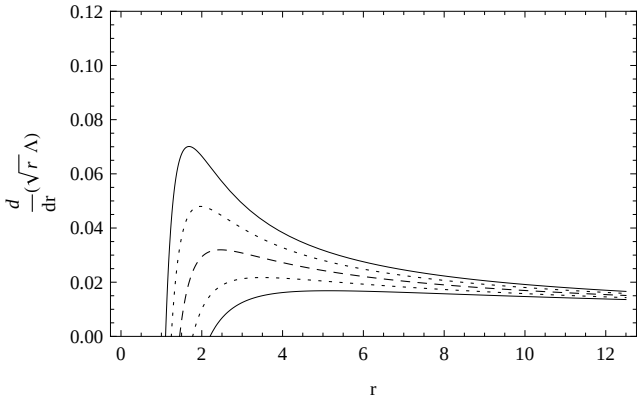

Figure 8. $\frac{d}{dr}\left(\sqrt{r}\Lambda\right)$ as a function of r for the fiducial neutron star with an accretion rate of $1.5 \times 10^{14}\,\mathrm{kg\,s^{-1}}$, and with $\epsilon = 0.1,\ 0.05,\ 0,\ -0.05,$ and -0.1 from the bottom to the top.

the $\epsilon = -0.12$ disc (Fig. 6), at which point the flow stagnates (Fig. 7). In the case V solutions, on the other hand, we see that $\Sigma \to 0$ at a point which is inside the inner edge of the disc (Fig. 8).

5 DISCUSSION

5.1 The inner edge of the accretion disc

In order for the neutron star to appear as an X-ray pulsar the accretion disc must be truncated by the stellar magnetic field (Tab. 2) at a radius R_0 outside of the neutron star. The inner edge of the disc can be either of type D ($\Lambda = 0$) or type V ($\frac{\mathrm{d}}{\mathrm{d}r}(\sqrt{r}\Lambda) = 0$) (see Paper I for an extensive discussion of these boundaries). In models without a dynamo (for instance Ghosh & Lamb 1979) R_0 is comparable to or smaller than the Alfvén radius, R_A, but we find that the dynamo can make it significantly larger than R_A. This opens up the possibility, as suggested by the referee, that a system can temporarily turn into an X-ray pulsar during the periods when the magnetic field generated by the dynamo is strong enough to make R_0 larger than the radius of the neutron star. SAX J1748.9-2021 is such an intermittent millisecond X-ray pulsar (Altamirano et al. 2008), which is on for hundreds of seconds at a time.

In case R_0 is located in the outer or middle region of our disc solution we find that a type D boundary coincides with the point at which $\rho \to 0$ and $v_R \to \infty$ though the accretion rate is finite. However a type D boundary in the inner part of the accretion disc behaves in the opposite way; $\rho \to \infty$ and $v_R \to 0$. Neither one of these behaviours is entirely physical and one must keep in mind that we have ignored the importance of the radial pressure gradient and the inertial term in Eq. (3) (see for instance Abramowicz et al. 1988; Popham & Narayan 1992), and we have not attempted to model how the plasma is entering the stellar magnetic field lines to form a funnel flow onto the magnetic poles of the neutron star. One further problem with the inner region of the disc solution is that it is known to be viscously and thermally unstable (Lightman & Eardley 1974). This instability persists if the accretion disc is threaded by a stellar magnetic field (Campbell 1998), but so far it has not been investigated what happens if the accretion disc is sustaining its own magnetic field through a dynamo.

5.2 Accretion torque

To understand the nature of the exchange of angular momentum between the accretion disc and the neutron star we multiply Eq. (14) by $2\pi R$ and integrate it from R_0, the inner radius of the disc, to a large radius R_1.

$$-\dot{M}\left(\sqrt{GMR_1}-\sqrt{GMR_0}\right)= \int_{R_0}^{R_1} 4\pi\frac{B_z B_{\phi,\rm dyn}}{\mu_0}R^2{\rm d}R+\int_{R_0}^{R_1} 4\pi\frac{B_z B_{\phi,\rm shear}}{\mu_0}R^2{\rm d}R -3\pi(\nu\Sigma)_{R_1}\sqrt{GMR_1}+3\pi(\nu\Sigma)_{R_0}\sqrt{GMR_0}. \quad (61)$$

The left-hand-side is the difference between the angular momentum that is advected through the inner edge of the accretion disc and that which is fed into the disc at its outer edge and the right-hand-side describes the contribution of magnetic and viscous torques to the angular momentum balance. Notice that the term $3\pi(\nu\Sigma)_{R_1}\sqrt{GMR_1}$ describes the viscous tension at the outer edge of the disc, which will not be considered further in this paper. The material torque of the inner edge of the disc on the neutron star is

$$N_{adv}=\dot{M}\sqrt{GMR_0}=1.4\times10^{26}\mu_{16}^{2/7}M_1^{3/7}\dot{M}_{14}^{6/7}r_0^{1/2}. \quad (62)$$

It increases as the accretion rate increases (Tab.2). Then we have the magnetic torques on the neutron star, which we have divided into one part due to the shear

$$N_{\rm shr}=-\int_{R_0}^{R_1}4\pi\frac{B_z B_{\phi,\rm shear}}{\mu_0}R^2{\rm d}R\approx 3.6\times10^{26}\gamma\mu_{16}^{2/7}M_1^{3/7}\dot{M}_{14}^{6/7}\int_{r_0}^{\infty}\left[r^{-4}\left(1-\omega_s r^{3/2}\right)\right]{\rm d}r \quad (63)$$

and a second part due to the dynamo

$$N_{\rm dyn}=-\int_{R_0}^{R_1}4\pi\frac{B_z B_{\phi,\rm dyn}}{\mu_0}R^2{\rm d}R. \quad (64)$$

We split up the latter integral into one integral for each of the three different regions of the disc

$$N_{\rm dyn,outer}=7.7\times10^{27}\epsilon\gamma_{dyn}^{1/2}\alpha_{\rm ss}^{1/20}\bar{\mu}^{3/16}\mu_{16}^{1/4}M_1^{5/8}\dot{M}_{14}^{4/5}\int_{\rm outer}\Lambda^{17/40}r^{-37/16}dr, \quad (65)$$

$$N_{\rm dyn,mid}=6.3\times10^{27}\epsilon\gamma_{dyn}^{1/2}\alpha_{\rm ss}^{1/20}\bar{\mu}^{1/5}\mu_{16}^{19/70}M_1^{17/28}\dot{M}_{14}^{107/140}\int_{\rm middle}\Lambda^{2/5}r^{-91/40}dr, \quad (66)$$

and

$$N_{\rm dyn,inner}=6.6\times10^{26}\epsilon\gamma_{dyn}^{1/2}\mu_{16}^{4/7}M_1^{5/14}\dot{M}_{14}^{3/14}\int_{\rm inner}r^{-7/4}dr. \quad (67)$$

Finally we have the boundary terms describing the viscous stresses on the inner and the outer edges of the accretion disc. The viscous stress at the outer edge of the disc is responsible for removing the angular momentum that is transported outwards through the accretion disc, and does not affect the angular momentum evolution of the neutron star. The viscous stress at the inner edge of the disc on the other hand can result in a torque that transports angular momentum away from the neutron star

$$N_{\rm vis}=-3\pi(\nu\Sigma)_{R_0}\sqrt{GMR_0}= -1.29\times10^{27}\mu_{16}^{2/7}M_1^{3/7}\dot{M}_{14}^{6/7}\Lambda(r_0)r_0^{1/2} \quad (68)$$

This term is usually neglected in accretion disc theory since the standard accretion disc solution has a case D inner boundary. But it can transport angular momentum from the neutron star to the disc when we have a case V inner boundary.

We report on all the components and the total sum of the torques on our fiducial neutron star in Tab.2. The main factor determining the total torque is the accretion rate. In Paper I we found that the dominant contributor to the torque is the internal disc dynamo. This torque is still strong, but now $N_{\rm adv}$ and $N_{\rm vis}$ are comparable in strength, though these make opposing contributions to the net torque, while the contribution from $N_{\rm sh}$ is still small. There is therefore no simple dependence of $N_{\rm total}$ on ϵ, though the dynamo is indirectly affecting $N_{\rm adv}$ and $N_{\rm vis}$ by causing the inner disc edge to move outwards compared to the Ghosh & Lamb (1979) model. $N_{\rm vis}$ is also highly sensitive to the nature of the inner disc boundary, and in particular it vanishes for a D inner boundary, which occurs at a sufficiently negative ϵ, in which case the net torque is determined by the balance between $N_{\rm dyn}$ and $N_{\rm adv}$.

5.3 Observed properties of millisecond X-ray Pulsars

The largest spin up rate recorded so far for a millisecond X-ray pulsar is $\sim 10^{-12}\,{\rm Hz\,s^{-1}}$ during the December 2004 outburst of IGR J00291+5934 (Burderi et al 2007), but one should keep in mind that there are large uncertainties in the spin variations that have been reported for the millisecond X-ray pulsars. For instance Burderi et al (2006) reported $\dot{\nu}$s between -7.6×10^{-14} and $4.4\times10^{-13}\,{\rm Hz\,s^{-1}}$ for SAX J1808.4-3658, but Hartman et al. (2008) noted that the measurements of this source are plagued by large variations in the pulse shape, and put an upper limit of $2.5\times10^{-14}\,{\rm Hz\,s^{-1}}$ on the spin variations at any instant. Some of the timing noise in the millisecond X-ray pulsars can be explained by the motion of the hot spot on the neutron star (Patruno et al. 2009), and may thus not correspond to real changes in the spin period of the neutron star.

The spin variation corresponds to a torque

$$N=2\pi\dot{\nu}I=6.3\times10^{25}\dot{\nu}_{13}I_{38}\,{\rm Nm}, \quad (69)$$

where I_{38} is the moment of inertia of the neutron star measured in $10^{38}\,{\rm kg\,m^2}$, and $\dot{\nu}_{13}$ is the spin derivative in units of $10^{-13}\,{\rm Hz\,s^{-1}}$. In the Ghosh & Lamb (1979) model, the spin variation of IGR J00291+5934 would imply then an accretion rate of at least $\sim 10^{14}\,{\rm kg\,s^{-1}}$, which is uncomfortably large, but our Tab. 2 shows that it is possible to enhance the torque severalfold by coupling the stellar magnetic field to the magnetic field generated by an internal dynamo in the disc, and through the fact that the inner edge of the accretion disc is then located outside the Alfvén radius, which increases the amount of angular momentum that is advected onto the neutron star. Thus it is possible that a lower accretion rate can produce the necessary torque, though we have not attempted to fit our model to this system.

5.4 The validity of the model

A significant part of the luminosity is not generated in the accretion disc outside of R_0, but rather it is released as the accreting matter falls onto the neutron star. We estimate that this luminosity is

$$L_{\rm NS}=GM\dot{M}\left(\frac{1}{R_{\rm NS}}-\frac{1}{R_0}\right)+\frac{1}{2}\frac{GM\dot{M}}{R_0}=GM\dot{M}\left(\frac{1}{R_{\rm NS}}-\frac{1}{2R_0}\right), \quad (70)$$

where we have assumed that both the potential energy difference between the inner edge of the accretion disc and the surface of the

Table 2. The inner edge of the accretion disc and its torque on the fiducial neutron star for different accretion rate.

$\dot{M}_{14}$	ϵ	$R_0\,[m]$	$N_{\rm dyn,outer}$ [Nm]	$N_{\rm dyn,Middle}$ [Nm]	$N_{\rm dyn,inner}$ [Nm]	$N_{\rm sh}$ [Nm]	$N_{\rm adv}$ [Nm]	$N_{\rm vis}$ [Nm]	$N_{\rm total}$ [Nm]
0.012	0.1	1.8×10^{5}	3.4×10^{24}	–	–	-7.8×10^{23}	7.0×10^{24}	-7.4×10^{24}	2.2×10^{24}
	0.05	9.9×10^{4}	3.7×10^{24}	–	–	-1.7×10^{24}	5.2×10^{24}	-6.7×10^{24}	5.0×10^{23}
	0	4.7×10^{4}	0	–	–	-3.1×10^{24}	3.6×10^{24}	-3.4×10^{22}	4.7×10^{23}
	−0.05	8.8×10^{4}	-2.9×10^{24}	–	–	-1.9×10^{24}	4.9×10^{24}	0	1.0×10^{23}
	−0.1	1.2×10^{5}	-4.1×10^{24}	–	–	-1.4×10^{24}	5.6×10^{24}	0	1.0×10^{23}
0.12	0.1	9.4×10^{4}	8.4×10^{25}	1.4×10^{25}	-	-2.1×10^{24}	5.1×10^{25}	-1.0×10^{26}	4.7×10^{25}
	0.05	6.0×10^{4}	4.1×10^{25}	1.5×10^{25}	-	-3.2×10^{24}	4.1×10^{25}	-7.7×10^{25}	1.7×10^{25}
	0	3.0×10^{4}	0	0	-	-7.4×10^{23}	2.9×10^{25}	-2.4×10^{25}	4.3×10^{24}
	−0.05	3.2×10^{4}	-4.0×10^{25}	-2.6×10^{25}	-	-2.0×10^{24}	2.9×10^{25}	-6.7×10^{22}	-3.9×10^{25}
	−0.1	4.8×10^{4}	-7.9×10^{25}	-3.0×10^{25}	-	-3.7×10^{24}	3.6×10^{25}	0	-7.7×10^{25}
0.8	0.1	3.2×10^{4}	4.9×10^{24}	3.1×10^{23}	8.2×10^{25}	-1.0×10^{25}	2.0×10^{26}	-2.7×10^{26}	7.2×10^{24}
	0.05	1.6×10^{4}	2.5×10^{24}	3.2×10^{25}	1.1×10^{26}	2.7×10^{25}	1.4×10^{26}	-2.5×10^{26}	6.2×10^{25}
	0	1.7×10^{4}	0	0	0	1.4×10^{25}	1.5×10^{26}	-1.6×10^{26}	4.0×10^{24}
	−0.05	2.0×10^{4}	-2.4×10^{24}	8.3×10^{22}	-7.7×10^{25}	2.5×10^{23}	1.6×10^{26}	-6.2×10^{25}	1.9×10^{25}
	−0.1	1.7×10^{4}	-4.8×10^{24}	-1.3×10^{25}	-1.8×10^{26}	1.4×10^{25}	1.4×10^{26}	0	-4.4×10^{25}
	−0.12	1.8×10^{4}	-5.8×10^{24}	-8.4×10^{24}	-2.0×10^{26}	-3.2×10^{24}	1.5×10^{26}	0	-6.7×10^{25}
1.5	0.1	2.6×10^{4}	2.1×10^{24}	2.5×10^{25}	1.1×10^{26}	-5.6×10^{24}	3.3×10^{26}	-4.5×10^{26}	1.2×10^{25}
	0.05	2.1×10^{4}	1.0×10^{24}	1.3×10^{25}	7.1×10^{25}	4.6×10^{24}	2.9×10^{26}	-4.2×10^{26}	-4.0×10^{25}
	0	1.8×10^{4}	0	0	0	1.7×10^{25}	2.7×10^{26}	-3.2×10^{26}	-3.3×10^{25}
	−0.05	1.6×10^{4}	-1.1×10^{24}	-1.3×10^{25}	-9.1×10^{25}	3.7×10^{25}	2.6×10^{26}	-3.2×10^{26}	-1.3×10^{26}
	−0.1	1.5×10^{4}	-2.1×10^{24}	-2.5×10^{25}	-2.0×10^{26}	5.5×10^{25}	2.5×10^{26}	-1.1×10^{25}	6.7×10^{25}
	−0.12	1.3×10^{4}	-2.5×10^{24}	-3.0×10^{25}	-2.4×10^{26}	5.8×10^{25}	2.5×10^{26}	0	3.6×10^{25}

neutron star as well as the kinetic energy associated with the Keplerian motion at the inner edge of the accretion disc is released at the surface of the neutron star. Consequently $GM\dot{M}/2R_{\rm NS} \le L_{\rm NS} \le GM\dot{M}/R_{\rm NS}$.

The neutron star can then contribute to the local heating in the accretion disc through its irradiation of the disc. Assuming that the neutron star is a point source and the accretion disc is flaring, i.e. $\mathrm{d}\ln H/\mathrm{d}\ln R > 0$, the irradiation flux on the accretion disc is at most (Frank, King & Raine 2002)

$$F_{\rm irr} = \frac{L_{\rm NS}}{4\pi R^2}\frac{H}{R}\left(\frac{\mathrm{d}\ln H}{\mathrm{d}\ln R}-1\right)(1-\beta) = \frac{GM\dot{M}}{4\pi R_{\rm NS}R^2}\frac{H}{R}\left(\frac{\mathrm{d}\ln H}{\mathrm{d}\ln R}-1\right)(1-\beta), \quad (71)$$

where β is the disc albedo (for a more complete treatment taking into account shadowing by the disc see Adams & Shu 1986). The local flux generated by the viscous heating in the accretion disc is on the other hand

$$F_{\rm accr} = \frac{9}{8}\frac{GM\nu\Sigma}{R^3}. \quad (72)$$

We thus find that

$$\frac{F_{\rm irr}}{F_{\rm accr}} = \frac{2}{3}\frac{H}{R_{\rm NS}}\left(\frac{\mathrm{d}\ln H}{\mathrm{d}\ln R}-1\right)(1-\beta), \quad (73)$$

and since $\mathrm{d}\ln H/\mathrm{d}\ln R - 1 \sim 0.1$ we find that irradiation dominates for $H \gtrsim 15R_{\rm NS}$ if $\beta = 0$. Consequently irradiation dominates over viscous heating for $R \gtrsim 10^4$ km. Thus the outer part of the accretion disc is hotter than is predicted by our model, which can be observed as an increased UV flux (Vrtilek et al. 1990). Thus we have underestimated the pressure in the outer disc, and since we have used the Shakura & Sunyaev (1973) prescription $\alpha_{\rm ss}P$ to estimate $B_{\phi,\rm dyn}$, we have also underestimated $B_{\phi,\rm dyn}$ and the torque from the outer disc on the neutron star. However, this torque is small in comparison to the total torque on the neutron star since $B_z B_{\phi,\rm dyn}$ is a rapidly decreasing function of R, and thus the effect of the irradiation of the outer disc does not significantly change our results. Irradiation is unlikely to significantly affect the inner disc, but, as pointed out above, other effects, such as radial advection and the transition from a disc flow to a funnel flow, that are not considered in this paper become important in the inner disc. We will investigate these effects in the future.

6 CONCLUSIONS

The accretion rates that have been observed in millisecond X-ray pulsars cover several orders of magnitude, and the highest accretion rates are sufficient that the innermost part of the accretion disc is dominated by radiation pressure and electron scattering. For these reasons we have followed the approach by Shakura & Sunyaev (1973) and divided our disc model in three regions, an outer region dominated by gas pressures and Kramer's opacity, a middle region dominated by gas pressure and electron scattering, and an inner region dominated by radiation pressure and electron scattering.

The large spin changes that have been observed in some of the accreting millisecond X-ray pulsars are difficult to explain in the model by Ghosh & Lamb (1979), but the inclusion of a disc dynamo produces a significant enhancement of the torque between the accretion disc and the neutron star. This increase is not only due to the coupling between the magnetic fields of the neutron star and the accretion disc as such, but also to the fact that the accretion disc is truncated at a larger radius thus increasing the lever arm between the edge of the disc and the neutron star.

ACKNOWLEDGMENTS

SBT thanks the Department of Physics at the University of Gothenburg for their hospitality and support during a part of this project. SBT is supported in part by the Swedish Institute (SI) under their Guest Scholarship Program. This research has made use of NASA's Astrophysics Data System. We thank an anonymous referee for comments that have improved the quality of the paper. We have also benefitted from discussions with Dr. Jonathan Ferreira.

REFERENCES

Abramowicz, M. A., Czerny, B., Lasota, J. P., & Szuszkiewicz, E. 1988, ApJ, 332, 646
Adams, F. C., & Shu, F. H. 1986, ApJ, 308, 836
Altamirano, D., Casella, P., Patruno A., Wijnands, R., & van der Klis, M. 2008, ApJ, 674, L45
Balbus S. A., & Hawley J. F., 1998, Rev. Mod. Phys., 70, 1
Brandenburg, A., Nordlund, A & A ., Stein, R. F. & Torkelsson U., 1995, ApJ, 446, 741
Burderi et al., 2006, ApJ, 653, L133
Burderi et al., 2007, ApJ, 657, 961
Campbell, C.G., 1998, MNRAS, 301, 754
Chakrabarty,D., & Morgan, E.H., 1998, Nature, 394, 346
Frisch, U., Pouquet, A., Leorat, J., & Mazure, A. 1975, JFM, 68, 769
Frank, J. King, A., & Raine, D. 2002, Accretion power in astrophysics, Cambridge University Press
Ghosh, P., & Lamb, F.K.,1979, ApJ, 232, 259 & ApJ, 234, 296
Hartman, J. M. et al. 2008, ApJ, 675, 1468
Hawley, J. F., Gammie, C. F., & Balbus, S. A. 1995, ApJ, 440, 742
Illarionov, A. F. & Sunyaev, R. A., 1975, A&A, 39, 185
Lightman, A. P., & Eardley, D. M., 1974, ApJ, 187, 1274
Long al et.,2008, MNRAS, 386, 1274
Matthews et al.,2004, MNRAS, 356, 66
Patruno, A., Wijnands, R., van der Klis, M., 2009, ApJ, 698, L60
Popham, R., & Narayan, R. 1992, ApJ, 394, 255
Rappaport S.A., Fregeau J.M., & Spruit H., 2004, ApJ, 606, 436
Romanova, M. M., Ustyugova, G. V., Koldoba, A. V., Lovelace, R. V. E., 2009, MNRAS, 399, 1802
Shakura N.I., & Sunyaev R.A., 1973, A&A, 24, 337
Shakura N.I., & Sunyaev R.A., 1976, MNRAS, 175, 613
Shapiro S.L, & Teukolsky S.A, 1983, Black holes, white dwarfs, and neutron stars. The Physics of Compact Objects, John Wiley & Sons, New York
Spruit H.C., & Taam R.E., 1993, ApJ, 402, 593
Tessema, S.B., & Torkelsson, U., 2010, A& A, 509, 45
Torkelsson, U. 1998, MNRAS, 298, L55
Torkelsson, U., & Brandenburg, A. 1994, A&A, 283, 677
Vrtilek, S. D., et al. 1990, A&A, 235, 162
White, N.E., & Stella,L., 1988, MNRAS, 231, 325
Wijnands,R., & van der Klis, M., 1998, Nature, 394, 344
Wijnands, R., 2004, Nucl. Phys. B Proc. Suppl., 132, 496